

Performance Comparison Between A Simple Full-Duplex Multi-Antenna Relay And A Passive Intelligent Reflecting Surface

Armin Bazrafkan, Marija Poposka, Zoran Hadzi-Velkov, Petar Popovski,
and Nikola Zlatanov

Abstract

In this paper, we propose a single RF-chain multi-antenna full-duplex (FD) relay built with b -bit analog phase shifters and passive self-interference cancellation. The hardware complexity of the proposed FD relay with 2-bit quantized analog phase shifters is on the same order as the hardware complexity of a passive intelligent reflecting surface (IRS). Next, assuming only passive self-interference cancellation at the FD relay, we derive the achievable data rate of a system comprised of a source, the proposed FD relay, and a destination. We then compare the achievable data rate of the proposed FD relaying system with the achievable data rate of the same system but with the FD relay replaced by an ideal passive IRS. Our results show that the proposed relaying system with 2-bit quantized analog phase shifters can significantly outperform the IRS-assisted system. Intuitively, the IRS system is in disadvantage since there the total transmit power P_T is used entirely by the source, whereas in the FD relaying system

A. Bazrafkan and N. Zlatanov are with the Department of Electrical and Computer Systems Engineering, Monash University, Melbourne, VIC, Australia. E-mails: (armin.bazrafkan, nikola.zlatanov)@monash.edu.

M. Poposka and Z. Hadzi-Velkov are with the Faculty of Electrical Engineering and Information Technologies, Ss. Cyril and Methodius University, 1000 Skopje, Macedonia. E-mails: (poposkam, zoranhv)@feit.ukim.edu.mk.

P. Popovski is with Department of Electronic Systems, Aalborg University, Denmark. E-mail: petarp@es.aau.dk.

the total power P_T is shared by the source and the FD relay in addition to the noise-cleansing process performed by the decode-and-forwarding at the FD relay.

Index Terms

Full-duplex relay, intelligent reflecting surface, performance comparisons.

I. INTRODUCTION

To meet the ever growing demands for wider bandwidths, the emerging wireless communication standards need to work in higher frequency bands, such as the millimetre (mmWave, 30-100 GHz) and the sub-millimetre (above 100 GHz) bands. Wireless transmission in these bands typically necessitates either a direct line-of-sight (LoS) between the transmitter and the receiver, or an intermediary device with a LoS to both the transmitter and the receiver. The intermediary device may be a conventional relay or a recent alternative known as an intelligent reflecting surface (IRS) [1], [2]. An IRS is an electronic surface comprised of reflecting meta elements, where each element can reflect the incoming electromagnetic wave and shift its phase such that the overall reflected signal from the IRS is beamformed towards a desired direction. In that sense, the IRS resembles a full-duplex (FD) amplify-and-forward relay with a large planar antenna array.

The recent influx of research papers on IRS-aided communications is attributed to the perceived advantages of this technology over conventional relaying [3]. Although the perception of an IRS outperforming conventional relaying is valid for half-duplex (HD) relaying, as shown in [4], it is yet unclear whether it is also valid for a practical multi-antenna FD relay. Certainly, this perception is not valid for an ideal FD relay that exhibits zero self-interference and has the same number of antenna elements as the IRS. However, an ideal FD relay is impractical to build in the real-world since it would require the same number of RF-chains as the number of antenna elements and a sophisticated

self-interference cancellation hardware. The natural question in this case is whether an IRS can outperform a massive-antenna FD relay with comparable design complexity. More specifically, can an IRS outperform a practical FD relay with the same number of antenna elements as the IRS but built only with one RF-chain on the receive side and one RF-chain on the transmit side? The aim of this paper is to answer this question. To the best of authors' knowledge, the performance of a single RF-chain multi-antenna FD relay has not been compared to the performance of a passive IRS-assisted system yet.

Massive antenna-arrays is the main technology that can significantly increase the spectral efficiency of mmWave communication systems [5], [6]. One of the most practically-plausible solutions for building massive antenna-arrays that exhibit low power consumption and low complexity is by adopting analog beamforming [7]–[10]. Analog beamforming can be implemented by equipping each antenna element with an analog phase-shifter, which can shift the phase of the transmitted/received signal by a desired phase, and thereby enable the massive-antenna array to perform transmit/receive beamforming to/from a desired direction in space. In general, there are many different technologies for building phase-shifters, such as reflective, loaded line, switched delay, Cartesian vector modulator, LO-path phase shifter, and phase-oversampling vector modulator [11]. Moreover, this is a very active field of research, with more-advanced phase-shifting technologies being constantly invented. One such technology has been recently proposed in [12], where the authors propose a low-cost 2-bit phase-shifter built using pin-diodes. Having in mind that the reflecting elements at the IRS are also built with pin-diodes [13], it can be concluded that a massive-antenna array built with 2-bit phase-shifters has a comparable cost as an IRS. As a result, a FD relay with separated transmit and receive massive-antenna arrays built with 2-bit phase shifters that only employs passive self-interference suppression has a comparable design complexity and implementation cost as an IRS. Relaying with large antenna arrays also has the potential to mitigate the self-interference in FD relays [14], [15].

In this paper, we first propose a simple single RF-chain multi-antenna FD relay implemented with b -bit analog phase shifters, where two different antenna arrays are used for transmission and reception, respectively, with passive self-interference suppression between them. Next, we derive an achievable data rate when the proposed FD relay is employed to relay the signal between a source and a destination. Finally, we compare the achievable data rate of the proposed FD relaying system with the achievable data rate of the same system but with the FD relay replaced by an ideal passive IRS. Our results show that the proposed relaying system with 2-bit quantized analog phase shifters can significantly outperform the IRS-assisted systems.

II. SYSTEM, FD RELAY, AND CHANNEL MODELS

In the following, we present the system model, the model of the proposed FD relay, and the channel models.

A. System Model

The system model is comprised of a single-antenna source transmitter, S , a single-antenna destination receiver, D , and an intermediary device that facilitates the transmission between the source and the destination. The intermediary device can either be a FD relay, as shown in Fig. 1 or an IRS, as shown in Fig. 2. The FD relay and the IRS are assumed to employ the same number of antenna elements. Next, both systems are assumed to use identical total transmit power P_T . In the case of the IRS system, the total power P_T is used entirely by the source, whereas in the FD relaying system the total power P_T is shared between the source, which uses power P_S , and the relay, which uses power P_R , such that $P_S + P_R = P_T$ holds.

We assume that the source and the destination cannot communicate directly due to physical obstacles, whereas the intermediary device has unobstructed LoS to both the

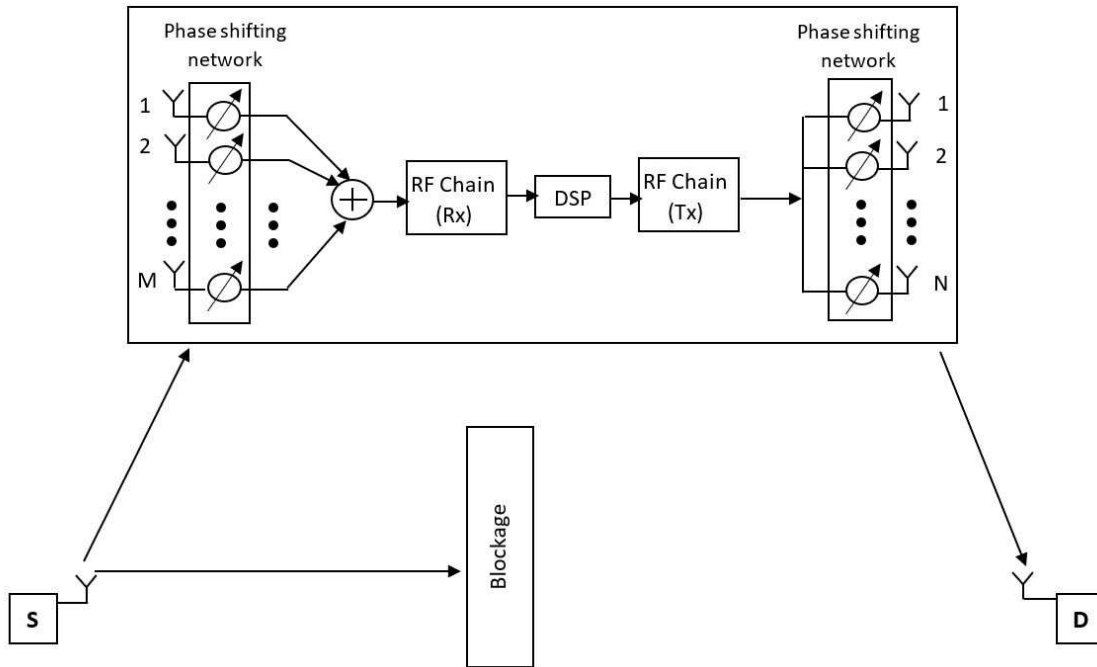


Fig. 1: Model of the full-duplex relay-assisted communications system.

source and the destination. As a result, the communication between the source and the destination must be conducted via the intermediary device, the FD relay or the IRS.

B. Model of the proposed FD relay

The relay in the relay-assisted communications system depicted in Fig. 1, is a massive-antenna FD decode-and-forward relay constructed as follows. The relay is comprised of two mutually isolated planar antenna arrays: (i) a receiving planar array with M antennas, and (ii) a transmitting planar array with N antennas, where $M + N = K$ and K is the total number of antenna elements at the FD relay. The receiving and transmitting planar arrays are only passively isolated, hence, there is no active self-interference cancellation used.

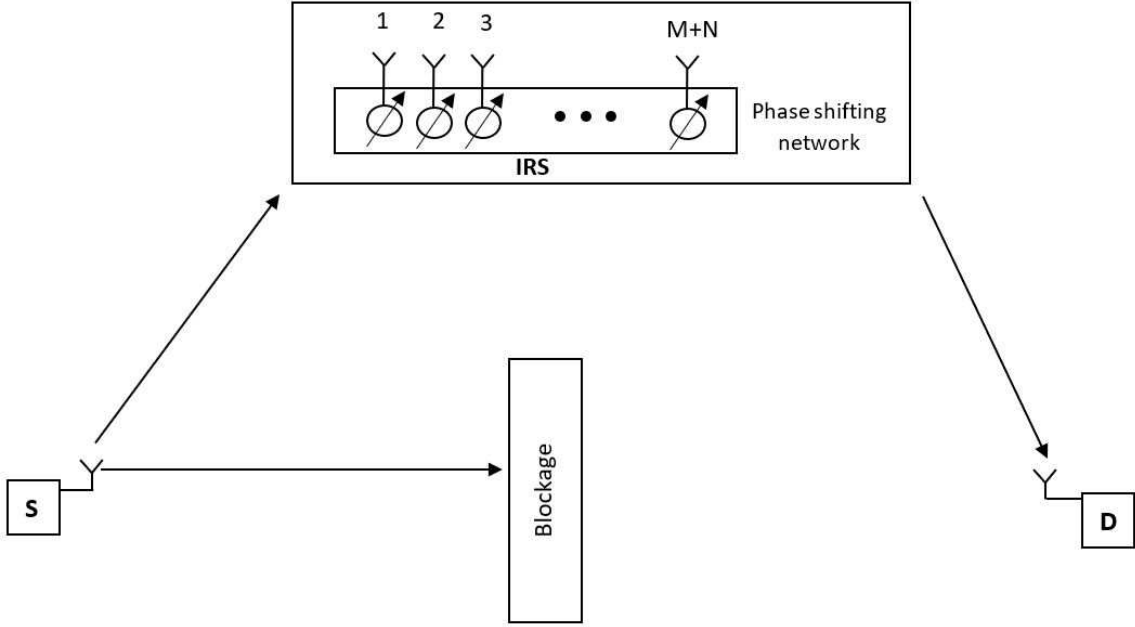


Fig. 2: Model of the IRS-assisted communications system.

As can be seen from the structure of the proposed FD relay illustrated in Fig. 1, the receive-side of the FD relay is comprised of M antennas, each connected to a b -bit analog phase shifter. The b -bit analog phase shifter can shift the phase of the received signal at the given antenna element by a phase from the following set

$$\mathcal{P} = \left\{ 0, \frac{2\pi}{2^b}, 2 \times \frac{2\pi}{2^b}, 3 \times \frac{2\pi}{2^b}, \dots, (2^b - 1) \times \frac{2\pi}{2^b} \right\}, \quad (1)$$

where $b = 1, 2, 3, \dots$. Next, the phase-shifted signals from each receive antenna are summed via an analogue combiner and sent to the receive RF-chain. The receive RF-chain obtains a baseband digital representation of its input signal, which is then sent to a digital signal processing (DSP) unit for digital processing.

On the transmit-side of the proposed FD relay, a digital transmit signal is sent to a transmit RF-chain, which produces a passband signal which is then fed into the N transmit antennas. Each transmit antenna is equipped with a b -bit analog phase shifter which shifts the phase of the transmit signal by a phase from the set \mathcal{P} in (1). The advantage of this transmit-side design is that only one common power amplifier is required for all transmit antennas.

The design in Fig. 1 is a fairly standard hardware design of massive antenna array systems with analog beamforming [7]–[10]. In fact, instead of conventional arrays, the proposed FD relay can be even build using reconfigurable holographic surfaces [16], [17].

1) *Channel Models*: Let the channel between the source and the receive-side of the FD relay be represented by the vector $\mathbf{h}_S = [h_{S,1}, h_{S,2} \cdots, h_{S,M}]^T$, where $h_{S,m}$ denotes the channel between the source and the relay's m -th receive antenna. Let the channel between the transmit-side of the FD relay and the destination be represented by the vector $\mathbf{h}_D = [h_{D,1}, h_{D,2} \cdots, h_{D,N}]^T$, where $h_{D,n}$ denotes the channel between the relay's n -th transmit antenna and the destination. The channels $h_{S,m}$ and $h_{D,n}$ are conventionally modelled as

$$h_{S,m} = \sqrt{\Omega_{S,m}} e^{j\phi_{S,m}} \quad (2)$$

$$h_{D,n} = \sqrt{\Omega_{D,n}} e^{j\phi_{D,n}}, \quad (3)$$

where $\Omega_{S,m}$ and $\phi_{S,m}$ denote the power gain and phase of the channel between the source and the relay's m -th receive antenna, whereas $\Omega_{D,n}$ and $\phi_{D,n}$ denote the power gain and phase of the channel between the relay's n -th transmit antenna and the destination. In mmWave bands, the channel is comprised of one very strong LoS component and few very weak non-LoS components. Thereby, each channel can be accurately modeled

as static with $\Omega_{S,m}$, $\Omega_{D,n}$, $\phi_{D,n}$ and $\phi_{S,m}$ fixed¹. We assume that the source and the destination are located in the far-field region of the relay, as defined in [18], and therefore, the corresponding channel power gains are given by [18]

$$\Omega_{S,m} = \Omega_S, \forall m, \quad (4)$$

$$\Omega_{D,n} = \Omega_D, \forall n. \quad (5)$$

2) *Relay's Self-Interference*: Due to the FD operation of the proposed relay, there is self-interference between the receive antenna array and the transmit antenna array. Despite the passive isolation, the relay's receiving antenna array is still exposed to residual self-interference from its transmit antenna array. In the following, we will derive the maximum amount of possible self-interference at the proposed FD relay.

Let $\mathbf{G} = [g_{mn}]_{M \times N}$ denote the self-interference channel matrix between the relay's transmit array and the relay's receive array, where g_{mn} is the self-interference channel between the n -th transmit antenna and the m -th receive antenna of the relay. As shown in [19], the worst-case scenario with respect to the achievable data rate of the proposed FD relaying system is when g_{mn} , $\forall m$ and $\forall n$, are independent and identically distributed (i.i.d.) zero-mean Gaussian random variables. In this paper, we adopt the worst-case scenario in terms of achievable rate for the proposed FD relaying system by assuming that $g_{mn} \sim \mathcal{CN}(0, \sigma_I^2)$, where σ_I^2 is the power gain of the self-interference channel between the n -th transmit antenna and the m -th receive antenna at the relay. In the following lemma, we obtain an upper bound on σ_I^2 , i.e., the highest possible value for the power gain of the self-interference channel.

Lemma 1. *In the absence of passive self-interference cancellation at the proposed relay, the power gain of the self-interference channel between any transmit antenna and any*

¹We note that in the case of Rayleigh fading, the channel parameters are not fixed anymore.

receive antenna at the proposed FD relay is upper bounded by

$$\sigma_I^2 \leq \frac{1}{M}. \quad (6)$$

Proof. Assuming the relay's transmit power, P_R , is equally allocated among the N transmit antennas, the average received power at the relay due to self-interference, P_I , is given by

$$\begin{aligned} P_I &= \frac{P_R}{N} E \left\{ \left| \sum_{m=1}^M \sum_{n=1}^N g_{mn} \right|^2 \right\} = \frac{P_R}{N} MN \sigma_I^2 \\ &= MP_R \sigma_I^2. \end{aligned} \quad (7)$$

Due to the law of conservation of energy, the average received power at the relay due to self-interference, P_I , must be smaller or equal to the relay's transmit power, P_R , i.e., $P_I \leq P_R$ must be satisfied. Combining (7) with $P_I \leq P_R$ yields (6). \square

We assume that a passive insulation is inserted between the relay's transmit and receive antenna arrays with a passive isolation coefficient η . In this case, (6) is transformed into $\sigma_I^2 \leq \eta/M$. Note, the typical values of the passive isolation coefficient vary between 10^{-6} and 10^{-5} , c.f. [20]. In the rest of the paper, we pessimistically set

$$\sigma_I^2 = \frac{\eta}{M}, \quad (8)$$

which leads to the lowest possible achievable data rate of the proposed FD relaying system.

C. Model of the passive IRS

The IRS-assisted communications system is depicted in Fig. 2. The IRS consists of K reflecting elements and has a total area R . Following [18], [21], [22], the IRS can be modelled as a planar antenna array, where each antenna element has an area of size

A , such that $R = KA$ and $A \leq (\lambda/4)^2$. The phase shift of each IRS element can be adjusted such that the incoming signal from the source is reflected and beamformed towards the destination. In order to facilitate the best possible performance of the IRS, we assume that each phase shifter at the IRS can be set to any value in the range $[0, 2\pi)$, i.e., opposite to the proposed FD relay, there is no phase quantization at the IRS. Note that the phase shifters at the IRS constitute a phase-shifting network [23].

Similar to the relay, we assume that the channel between S and the k -th reflective element at the IRS is denoted by $h_{S,k}$, and the channel between the k -th reflective element at the IRS and the destination is denoted by $h_{D,k}$. The channels $h_{S,k}$ and $h_{D,k}$, for $k = 1, 2, \dots, K$, are given by

$$h_{S,k} = \sqrt{\Omega_{S,k}} e^{j\phi_{S,k}} \quad (9)$$

$$h_{D,k} = \sqrt{\Omega_{D,k}} e^{j\phi_{D,k}}, \quad (10)$$

where $\Omega_{S,k}$ and $\phi_{S,k}$ denote the power gain and phase of the channel between the source and the IRS's k -th reflective element, whereas $\Omega_{D,k}$ and $\phi_{D,k}$ denote the power gain and phase of the channel between the IRS's k -th reflective element and the destination. Similar to the relaying system model, each channel is modeled as static with $\Omega_{S,k}$, $\Omega_{D,k}$, $\phi_{D,k}$, and $\phi_{S,k}$ being fixed $\forall k$. Moreover, again similar to the relaying system, we assume that the source and the destination are located in the far-field region of the IRS, as defined in [18], and therefore, the corresponding channel power gains are given by [18]

$$\Omega_{S,k} = \Omega_S, \forall k, \quad (11)$$

$$\Omega_{D,k} = \Omega_D, \forall k. \quad (12)$$

III. ACHIEVABLE DATA RATES

In this section, we derive the achievable data rate of the proposed FD relaying system as well as provide the achievable data rate of the IRS system.

A. Data Rate of the Relay-Assisted System

Let P_S denote the transmit power of the source and P_R denote the transmit power of the relay, where $P_S + P_R = P_T$ must hold and P_T is the total available power in the relaying system available for sharing between the source and the relay. Let x_S denote the signal transmitted by the source, such that $E\{|x_S|^2\} = P_S$. Let $\bar{\mathbf{y}}_R = [\bar{y}_{R,1}, \bar{y}_{R,2}, \dots, \bar{y}_{R,M}]^T$ denote the received signal vector at the relay, where $\bar{y}_{R,m}$ is the received signal at the m -th receive antenna of the relay before any phase shift is applied. The received vector $\bar{\mathbf{y}}_R$ is comprised of following three components: (i) the signal from the source that arrives via the channel \mathbf{h}_{SR} , given by $x_S \mathbf{h}_{SR}$, (ii) the noise vector at the relay, \mathbf{w}_R , and (iii) the self-interference vector, which is found in the following.

Let x_R denote the information signal of the relay, such that $E\{|x_R|^2\} = P_R$. Let $\mathbf{v} = [v_1, v_2, \dots, v_N]^T$ denote the phase shift vector of the relay's transmit antenna array. The relay's n -th transmit antenna transmits the signal $x_R v_n / \sqrt{N}$, where $v_n \in \mathcal{P}$ is the corresponding phase shift applied at this antenna. Thus, the self-interference vector at the relay is given by $x_R \mathbf{G} \mathbf{v} / \sqrt{N}$, whereas the received vector $\bar{\mathbf{y}}_R$ is given by

$$\bar{\mathbf{y}}_R = x_S \mathbf{h}_{SR} + \frac{1}{\sqrt{N}} x_R \mathbf{G} \mathbf{v} + \mathbf{w}_R. \quad (13)$$

In (13), $\mathbf{w}_R = [w_{R,1}, w_{R,2}, \dots, w_{R,M}]^T$ denotes the complex additive white Gaussian noise (AWGN) vector at the relay, where $w_{R,m} \sim \mathcal{CN}(0, N_0)$, for $m = 1, \dots, M$, is the complex AWGN at the m -th receive antenna of the relay.

Next, let $\mathbf{u} = [u_1, u_2, \dots, u_M]^T$ denote the phase shift vector of the relay's receive antenna array, where $u_m \in \mathcal{P}$ is the phase shift at the relay's m -th receive antenna. The

input signal to the relay's receive RF-chain is given by

$$\begin{aligned} y_R &= \mathbf{u}^T \bar{\mathbf{y}}_R \\ &= x_S \mathbf{u}^T \mathbf{h}_S + \frac{1}{\sqrt{N}} x_R \mathbf{u}^T \mathbf{G} \mathbf{v} + \mathbf{u}^T \mathbf{w}_R. \end{aligned} \quad (14)$$

The received signal at the destination is given by

$$y_D = \frac{1}{\sqrt{N}} x_R \mathbf{v}^T \mathbf{h}_D + w_D, \quad (15)$$

where $w_D \sim \mathcal{CN}(0, N_0)$ denotes the complex AWGN at the destination.

Having derived the input-output relationship of the proposed FD relaying system, we are now ready to derive its achievable data rate, which is provided in the following theorem.

Theorem 1. *When the phase shift vectors \mathbf{u} and \mathbf{v} are given by*

$$\mathbf{u} = [e^{-j\hat{\phi}_{S,1}}, e^{-j\hat{\phi}_{S,1}}, \dots, e^{-j\hat{\phi}_{S,M}}]^T \quad (16)$$

$$\mathbf{v} = [e^{-j\hat{\phi}_{D,1}}, e^{-j\hat{\phi}_{D,1}}, \dots, e^{-j\hat{\phi}_{D,N}}]^T, \quad (17)$$

where $\hat{\phi}_{S,m}$ and $\hat{\phi}_{D,n}$ are the b -bit quantized versions of the channel phases $\phi_{S,m}$ and $\phi_{D,n}$, respectively, and are given by

$$\begin{aligned} \hat{\phi}_{S,m} &= \frac{2m\pi}{2^b} \text{ if } \phi_{S,m} \in \left[\frac{2m\pi}{2^b}, \frac{2(m+1)\pi}{2^b} \right) \\ \hat{\phi}_{D,n} &= \frac{2m\pi}{2^b} \text{ if } \phi_{D,n} \in \left[\frac{2m\pi}{2^b}, \frac{2(m+1)\pi}{2^b} \right) \\ &\text{for } m \in \{0, 1, \dots, 2^b - 1\}, \end{aligned} \quad (18)$$

then the achievable data rate of the proposed FD relaying system is given by

$$\begin{aligned}
R = & \\
& \min \left\{ \log_2 \left(1 + \frac{P_S \Omega_{SR} (1 + (M - 1)Q)}{N_0 + \frac{\eta}{M} P_R} \right), \right. \\
& \left. \log_2 \left(1 + \frac{P_R \Omega_{RD} (1 + (N - 1)Q)}{N_0} \right) \right\}, \tag{19}
\end{aligned}$$

where

$$Q = \left(\frac{2^b}{\pi} \sin \left(\frac{\pi}{2^b} \right) \right)^2. \tag{20}$$

Proof. Please refer to the Appendix A. \square

Obviously, the data rate in (19) can be maximized by optimizing the values of M , N , P_S , and P_R , given the constraint $M + N = K$ and $P_R + P_S = P_T$. Specifically, the maximum achievable data rate of the proposed relaying system is obtained as

$$\begin{aligned}
& \max_{P_R, N} R \\
& \text{s.t. } M + N = K \\
& P_S + P_R = P_T, \tag{21}
\end{aligned}$$

where the objective function R is given in (19) and P_T is the total available power shared between the source and the relay.

Note that (21) can be easily transformed into an unconstrained optimization problem, which can then be solved numerically by conventional methods for optimization of differentiable functions, such as the steepest gradient descent method, or the Newton's method. However, this approach does not lead to a closed-form solution. In order to provide a closed-form solution of (21), we provide the following proposition.

Proposition 1. We propose the following sub-optimal solution of (21),

$$M^* = \frac{2K}{3}, \quad (22)$$

$$N^* = \frac{K}{3}, \quad (23)$$

$$P_R^* = \frac{-\alpha + \sqrt{48P_T K N_0 \eta \Omega_S \Omega_D + \alpha^2}}{6\eta \Omega_D}, \quad (24)$$

$$P_S^* = P_T - P_R^*, \quad (25)$$

where $\alpha = 2K N_0 \Omega_D + 4K N_0 \Omega_S$.

Proof. Please refer to the Appendix B. \square

Remark 2: The channel state information (CSI) required for obtaining the phase shift vectors \mathbf{u} and \mathbf{v} as per (16) and (17) is the b -bit quantized information of the phases of the source-relay and relay-destination channels, respectively. This b -bit quantized channel phase information can be acquired directly in the analog domain as per [24], [25], or by adapting any of the CSI acquisition methods developed for IRS-assisted networks. In that sense, the relay system does not waste more resources in acquiring the CSI than the corresponding IRS system.

B. Rate of the IRS-assisted system

Let P_T denote the transmit power of the source². Assuming static LoS channels from the source to the IRS and from the IRS to the destination, the achievable data rate between the source and destination, R_{IRS} , is given by [18, Eq. (48)]

$$R_{IRS} = \log_2 \left(1 + \frac{K^2 P_T \Omega_S \Omega_D}{N_0} \right). \quad (26)$$

²Note that the relaying system also consumes power P_T , however, the power P_T is shared between the source and the relay.

C. Rates in Rayleigh fading channel

The data rates for the relaying system in (19) and the IRS system in (26) hold for LoS and static fading. In the following, we provide the data rates for Rayleigh fading.

The corresponding expressions for the achievable data rates of the relaying and IRS systems in Rayleigh fading channel are determined by the following corollaries.

Corollary 1. *In Rayleigh fading, the achievable data rate of the proposed relay-assisted communications system, R^{Ra} , is given by*

$$R^{Ra} = \min \left\{ \log_2 \left(1 + \gamma_{SR}^{Ra} \right), \log_2 \left(1 + \gamma_{RD}^{Ra} \right) \right\}, \quad (27)$$

where

$$\begin{aligned} \gamma_{SR}^{Ra} &= \frac{P_S \Omega_S \left(1 + (M-1) \frac{\pi}{4} Q \right)}{N_0 + \frac{P_R}{N}} \\ \gamma_{RD}^{Ra} &= \frac{P_R \Omega_D \left(1 + (N-1) \frac{\pi}{4} Q \right)}{N_0}. \end{aligned} \quad (28)$$

Proof. Please refer to Appendix C. □

In Rayleigh fading, the achievable data rate of the considered IRS-assisted communications system is given by [26, Eq. (34)]

$$\begin{aligned} R_{IRS}^{Ra} &= \log_2 \left(1 + \frac{P_T \Omega_S \Omega_R K}{N_0} \right. \\ &\quad \left. \times \left(1 + (K-1) \left(\frac{\pi}{4} \right)^2 \right) \right). \end{aligned} \quad (29)$$

From (26) and (29), we can see that the Rayleigh fading reduces the signal-to-noise ratio (SNR) by the factor of $\pi/4$ with respect to the case of static fading. Furthermore,

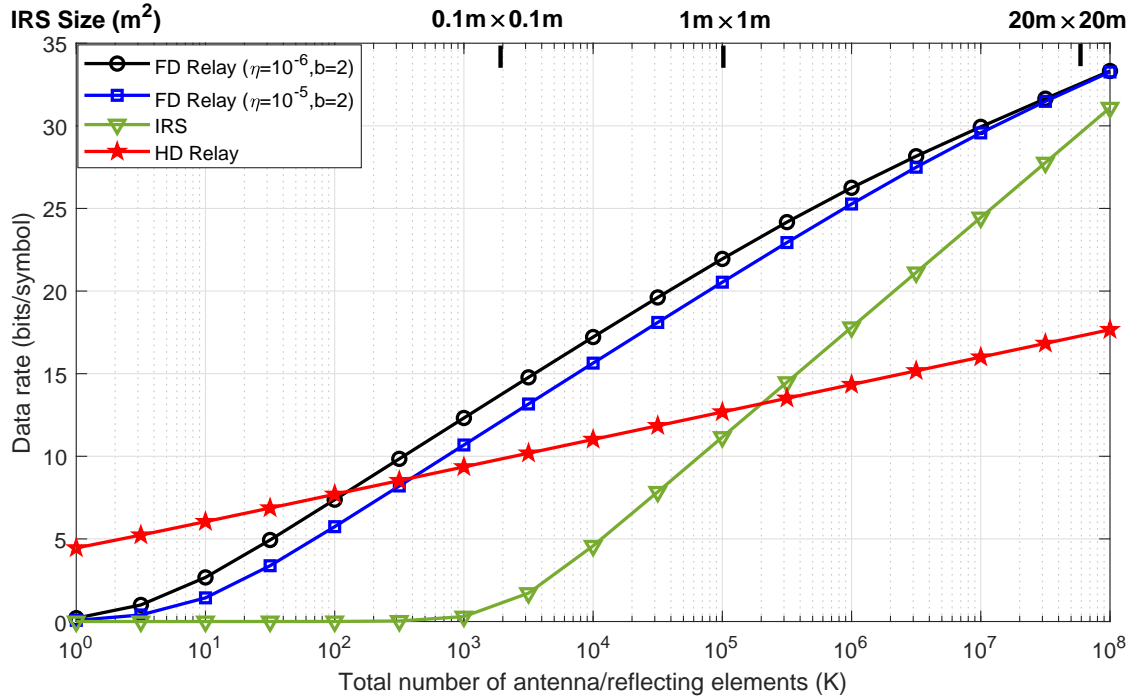


Fig. 3: Data rate as a function of the number of antenna elements K (LoS).

similarly to the rate (21), the rate (27) can be maximized by adopting the sub-optimal solutions in Proposition 1.

IV. NUMERICAL RESULTS

For fair comparison between the IRS-assisted system and the relay-assisted system, we adopt the planar array structure considered in [18] including the corresponding assumptions, and thereby assume the area of each transmit/receive antenna element at the relay and each reflecting element at the IRS, denoted by A , satisfies $A \leq (\lambda/4)^2$, where λ is the signal's carrier wavelength.

Let d_S denote the distances between the source and the IRS/Relay center and d_R denote the distance between the IRS/Relay center and the destination. According to [

[18], Eq. (11)], the far-field assumption is justified if the conditions $\sqrt{KA} \leq 3d_S$ and $\sqrt{KA} \leq 3d_R$ are met. In this case, $\Omega_{S,k}$ and $\Omega_{D,k}$ are respectively approximated by [18], Eq. (11) and Eq. (31)] as

$$\Omega_{S,k} \approx \frac{A \cos(\alpha_S)}{4\pi d_S^2} = \Omega_S, \forall k, \quad (30)$$

$$\Omega_{D,k} \approx \frac{A \cos(\alpha_D)}{4\pi d_D^2} = \Omega_D, \forall k. \quad (31)$$

In (30) and (31), α_S is the angle between the source and IRS/Relay LoS and the IRS/Relay boresight, and α_D is the angle between the destination IRS/Relay LoS and the IRS/Relay boresight.

We set the following system parameters: $\lambda = 0.01\text{m}$ (i.e., 30 GHz), $A = (\lambda/4)^2$, $d_S = 25\text{m}$, $\alpha_S = \pi/6$, $d_R = 10\text{m}$, and $\alpha_R = -\pi/6$. The total transmit power is $P_T = 1\text{W}$ while the thermal noise power is set to $N_0 = 10^{-12}\text{W}$. We assume that each analog phase shifter at the relay is a 2-bit phase shifter, which yields $\mathcal{P} = \{0, \frac{\pi}{2}, \pi, \frac{3\pi}{2}\}$.

Benchmark (Half-duplex relay): In the numerical results, we also present the achievable rate of a communication system assisted by a half-duplex (HD) relay. If instead of the FD mode, the relay works in the HD mode and uses all of its K antennas both for transmission and reception in different time slots, the achievable data rate of the corresponding HD relaying system is given by

$$R_{HD} = \frac{\log_2(1 + \gamma_{SR}^{HD}) \log_2(1 + \gamma_{SD}^{HD})}{\log_2(1 + \gamma_{SR}^{HD}) + \log_2(1 + \gamma_{SD}^{HD})}, \quad (32)$$

where

$$\begin{aligned} \gamma_S^{HD} &= \frac{P_T \Omega_S (1 + (K-1)Q)}{N_0} \\ \gamma_D^{HD} &= \frac{P_T \Omega_D (1 + (K-1)Q)}{N_0} \end{aligned} \quad (33)$$

Note, the proof is straightforward using the vast available literature on HD relaying, e.g.

[27].

The three considered rates are compared in Fig. 3 as a function of the total number of IRS/antenna elements K (bottom x -axis), as well as a function of the size of the IRS (top x -axis). As can be seen from Fig. 3, the FD relay significantly outperforms the IRS when the self-interference is either $\eta = 10^{-5}$ (i.e., 50 dB) or $\eta = 10^{-6}$ (i.e., 60 dB). In fact, for an IRS of size of $1\text{m} \times 1\text{m}$, the proposed FD relay achieves almost double the data rate of the IRS.

When K grows to $K = 10^8$ or larger, the destination starts to operate in the near field of the relay/IRS, in which case the IRS has a size larger than $20\text{m} \times 20\text{m}$ and therefore it can be considered that the relay/IRS is a part of the destination itself. As a result, in that range, the IRS does not outperform the FD relay, instead the two have identical performances since both can be considered as a part of the destination.

In Fig. 4, similar to Fig. 3, the achievable data rates of the proposed FD relay and the IRS have been compared under the same assumptions except instead of a LoS channel a Rayleigh fading channel has been assumed. By comparing Fig. 4 and Fig. 3, we can observe that in the case of Rayleigh fading, the proposed FD relay outperforms the IRS by a slightly larger margin compared to the case of LoS channel. This is because by comparing (19) with (27) and (26) with (29), it can be seen that the Rayleigh fading reduces the SNR of the relay by a factor of $\pi/4$ and the SNR of the IRS by a factor of $(\pi/4)^2$. Therefore, in the case of Rayleigh fading channel, the performance gain of the proposed FD relay compared to the IRS is even larger.

Fig. 5 compares the three considered data rates as a function of d_D when $d_S = 25\text{m}$ and when the same values as for Fig. 3 are used for the other parameters. Two sets of curves are presented, one for $K = 10^3$ and the other for $K = 10^6$ antenna elements. In both cases, the proposed FD relay significantly outperforms both the IRS and the HD relay.

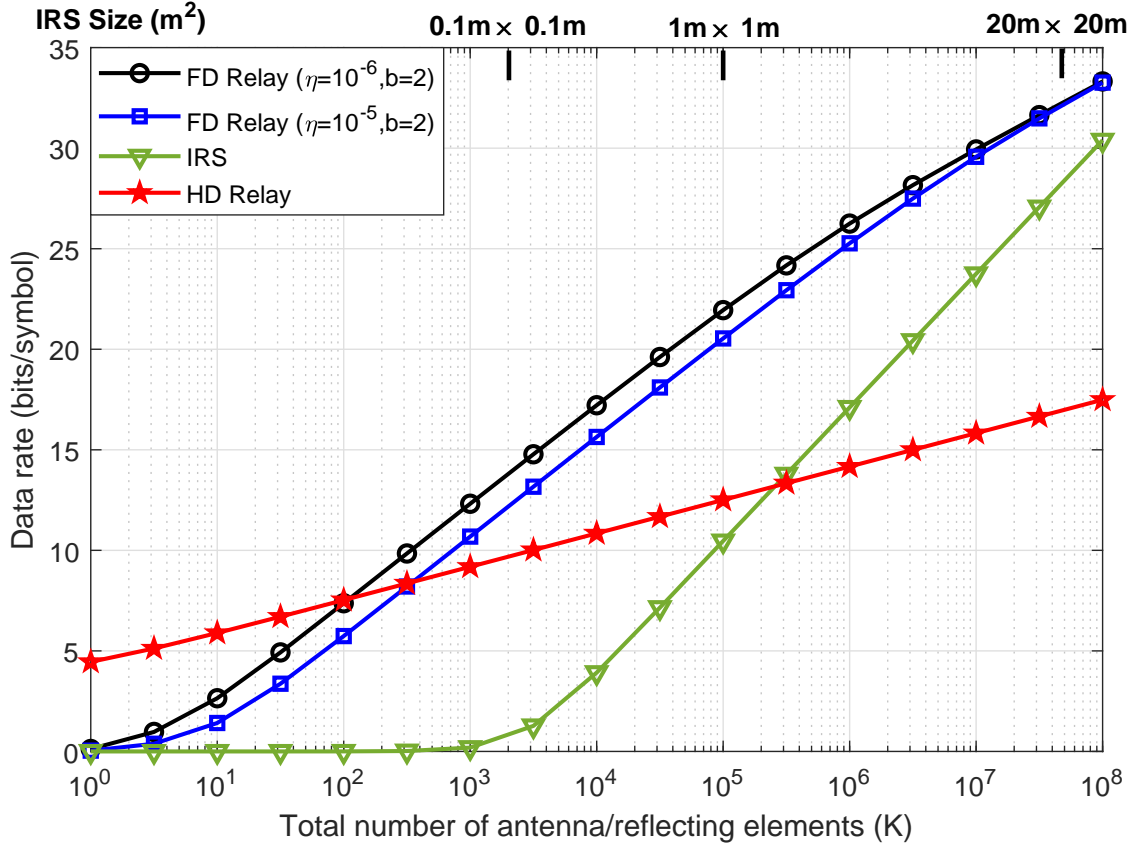


Fig. 4: Data rate as a function of the number of antenna elements K (Rayleigh).

V. CONCLUSION

We proposed a single RF-chain multi-antenna FD relay with discrete analog phase shifters that employs passive self-interference suppression. Next, we compared the achievable data rate of a system comprised of a source, the proposed FD relay, and a destination with the achievable data rate of the same system but with the FD relay replaced by an ideal passive IRS. We showed that the FD relaying system with 2-bit quantized analog phase shifters significantly outperforms the IRS system.

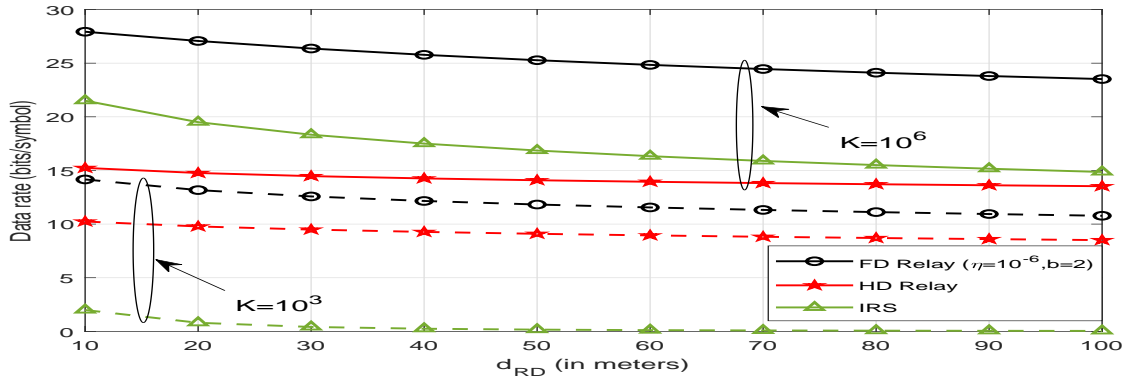


Fig. 5: Data rate as a function of the distance d_D .

APPENDIX A

PROOF OF THEOREM 1

As a result of (14), the signal-to-interference-plus-noise ratio (SINR) at the receive-side of the relay, denoted by γ_{SR} , is given by

$$\gamma_{SR} = \frac{E_{x_S} \{ |x_S \mathbf{u}^T \mathbf{h}_S|^2 \}}{E_{\mathbf{w}_R} \{ |\mathbf{u}^T \mathbf{w}_R|^2 \} + E_{x_R, \mathbf{G}} \left\{ \left| \sqrt{\frac{1}{N}} x_R \mathbf{u}^T \mathbf{G} \mathbf{v} \right|^2 \right\}}, \quad (34)$$

where the subscript of the expectations indicates the random variable(s) with respect to which the expectation is calculated. Now, we have $E_{x_S} \{ |x_S \mathbf{u}^T \mathbf{h}_S|^2 \} = P_S |\mathbf{u}^T \mathbf{h}_S|^2$,

which follows from $E_{x_S} \{|x_S|^2\} = P_S$. Next, when M is large, $|\mathbf{u}^T \mathbf{h}_S|^2$ is given by

$$\begin{aligned}
|\mathbf{u}^T \mathbf{h}_S|^2 &= \left| \sum_{m=1}^M \sqrt{\Omega_S} e^{j\bar{\phi}_{S,m}} \right|^2 \\
&= M\Omega_S + M(M-1)\Omega_S \\
&\quad \times \sum_{m=1}^M \sum_{j=1, j \neq m}^M \frac{e^{j\bar{\phi}_{S,m}} e^{-j\bar{\phi}_{S,j}}}{M(M-1)} \\
&= M\Omega_S + M(M-1)\Omega_S \\
&\quad \times E_m \{e^{j\bar{\phi}_{S,m}}\} E_j \{e^{-j\bar{\phi}_{S,j}}\} \stackrel{(b)}{=} M\Omega_S \\
&\quad + M(M-1)\Omega_S \left(\frac{2^b}{\pi} \sin \left(\frac{\pi}{2^b} \right) \right)^2, \tag{35}
\end{aligned}$$

where $\bar{\phi}_{S,m} = \phi_{S,m} - \hat{\phi}_{S,m}$, and (b) follows from the fact that $\bar{\phi}_{S,m}$ and $\bar{\phi}_{S,j}$ have uniform distributions over $[-\frac{\pi}{2^b}, \frac{\pi}{2^b})$. Moreover, the average power of the self-interference is given by

$$\begin{aligned}
&E_{x_R, \mathbf{G}} \left\{ \left| \sqrt{\frac{1}{N}} x_R \mathbf{u}^T \mathbf{G} \mathbf{v} \right|^2 \right\} \\
&\stackrel{(c)}{=} \frac{P_R}{N} E_{\mathbf{G}} \left\{ |\mathbf{u}^T \mathbf{G} \mathbf{v}|^2 \right\}, \tag{36}
\end{aligned}$$

where (c) results from $E_{x_R} \{|x_R|^2\} = P_R$. On the other hand, $E_{\mathbf{G}} \left\{ |\mathbf{u}^T \mathbf{G} \mathbf{v}|^2 \right\}$ is obtained as

$$\begin{aligned}
E_{\mathbf{G}} \left\{ |\mathbf{u}^T \mathbf{G} \mathbf{v}|^2 \right\} &= \sum_{m=1}^M \sum_{n=1}^N E_{\mathbf{G}} \{|g_{mn}|^2\} \\
&+ \sum_{m=1}^M \sum_{n=1}^N \sum_{i \neq m}^M \sum_{j \neq n}^N E_{\mathbf{G}} \{g_{mn}\} E_{\mathbf{G}} \{g_{ij}\} \\
&\times e^{-j\hat{\phi}_{S,m} \hat{\phi}_{S,i}} e^{-j\hat{\phi}_{D,n} \hat{\phi}_{D,j}} \\
&= \sum_{m=1}^M \sum_{n=1}^N E_{\mathbf{G}} \{|g_{mn}|^2\} = MN\sigma_I^2 \stackrel{(d)}{=} N\eta, \tag{37}
\end{aligned}$$

where (d) follows when $\sigma_I^2 \leq \frac{\eta}{M}$ holds with equality. Inserting (37) into (36), we obtain (36) as

$$E_{x_R, \mathbf{G}} \left\{ \left| \sqrt{\frac{1}{N}} x_R \mathbf{u}^T \mathbf{G} \mathbf{v} \right|^2 \right\} = P_R \eta. \tag{38}$$

Now, considering (38), (35), and the fact that $E_{\mathbf{w}_R} \left\{ |\mathbf{u}^T \mathbf{w}_R|^2 \right\} = MN_0$, we obtain γ_{SR} in (34) as

$$\begin{aligned}
\gamma_{SR} &= \frac{P_S \left(\Omega_S + (M-1)\Omega_S \left(\frac{2^b}{\pi} \sin \left(\frac{\pi}{2^b} \right) \right)^2 \right)}{N_0 + \frac{\eta}{M} P_R}. \tag{39}
\end{aligned}$$

On the other hand, from (15), the received SNR at the destination, denoted by γ_{RD} ,

is given by

$$\begin{aligned}\gamma_{RD} &= \frac{E_{x_R} \left\{ \left| \frac{1}{\sqrt{N}} x_R \mathbf{v}^T \mathbf{h}_D \right|^2 \right\}}{E_{w_D} \{w_D^2\}} \\ &\stackrel{(e)}{=} \frac{P_R |\mathbf{v}^T \mathbf{h}_D|^2}{NN_0},\end{aligned}\quad (40)$$

where (e) results from $E\{|x_R^2|\} = P_R$. In (40), $|\mathbf{v}^T \mathbf{h}_D|^2$ can be obtained by replacing N with M and Ω_D with Ω_S in (35). As a result, γ_{RD} is given by

$$\begin{aligned}\gamma_{RD} &= \\ &\frac{P_R \left(\Omega_D + (N-1)\Omega_D \left(\frac{2^b}{\pi} \sin \left(\frac{\pi}{2^b} \right) \right)^2 \right)}{N_0}.\end{aligned}\quad (41)$$

Finally, the achievable data rate is given by

$$R = \min \{ \log_2 (1 + \gamma_{SR}), \log_2 (1 + \gamma_{RD}) \}, \quad (42)$$

where γ_{SR} and γ_{RD} are given in (39) and (41), respectively, which leads to (19).

APPENDIX B

PROOF OF PROPOSITION 1

According to [27, Th1], in order to maximize the relay rate, the following needs to hold

$$\begin{aligned}&\frac{P_S \Omega_S (1 + (M-1)Q)}{N_0 + \frac{\eta}{M} P_R} \\ &= \frac{P_R \Omega_D (1 + (N-1)Q)}{N_0}\end{aligned}\quad (43)$$

On the other hand, since M and N are large numbers, we adopt the following highly accurate approximations: $1 + (M-1)Q \approx MQ$ and $1 + (N-1)Q \approx NQ$. Hence, (43)

transforms into

$$\frac{P_S \Omega_S M Q}{N_0 + \frac{\eta P_R}{M}} = \frac{P_R \Omega_D N Q}{N_0}. \quad (44)$$

Denoting $a = \frac{\Omega_S}{\Omega_D}$, and $\eta_0 = \frac{\eta}{N_0}$, we obtain the following equality from (44)

$$\eta_0 N P_R^2 + M N P_R - a M^2 P_S = 0. \quad (45)$$

Next, in order to maximize the relay SINR, we form the following optimization problem

$$\begin{aligned} & \max_{P_S, P_R, M, N} P_R N \\ \text{s.t. } & C_1 : \eta_0 N P_R^2 + M N P_R - a M^2 P_S = 0 \\ & C_2 : P_R + P_S = P_T \\ & C_3 : M + N = K. \end{aligned} \quad (46)$$

We use Lagrangian multipliers method to solve (46). Hence, the Lagrangian function is formed as

$$\begin{aligned} L = & P_R N + \lambda_1 (\eta_0 N P_R^2 + M N P_R - a M^2 P_S) \\ & + \lambda_2 (P_R + P_S - P_T) + \lambda_3 (M + N - K). \end{aligned} \quad (47)$$

We find the derivative of L with respect to P_R , P_S , M , and N and set them to zero as follows

$$\frac{dL}{dP_R} = N + 2\lambda_1 N \eta_0 P_R + \lambda_1 M N + \lambda_2 = 0 \quad (48)$$

$$\frac{dL}{dN} = P_R + \lambda_1 P_R^2 \eta_0 + M P_R \lambda_1 + \lambda_3 = 0 \quad (49)$$

$$\frac{dL}{dM} = \lambda_1 N P_R - 2\lambda_1 a M P_S + \lambda_3 = 0 \quad (50)$$

$$\frac{dL}{dP_S} = -\lambda_1 a M^2 + \lambda_2 = 0 \quad (51)$$

Let $a_{11} = N(2\eta_0 P_R + M)$, $a_{21} = P_R^2 \eta_0 + M P_R$, $a_{31} = N P_R - 2a M P_S$, and $a_{41} = -a M^2$. Hence, (48)-(51) can be written as

$$\begin{bmatrix} a_{11} & 1 & 0 \\ a_{21} & 0 & 1 \\ a_{31} & 0 & 1 \\ a_{41} & 1 & 0 \end{bmatrix} \begin{bmatrix} \lambda_1 \\ \lambda_2 \\ \lambda_3 \end{bmatrix} = \begin{bmatrix} -N \\ -P_R \\ 0 \\ 0 \end{bmatrix}. \quad (52)$$

The system of equations in (52) consists of four equations and three unknowns. Since we assume that there exists a unique solution, the four equations in (52) must be linearly dependent. Thus, the system determinant must be equal to zero. As a result, the following needs to hold

$$\begin{vmatrix} a_{11} & 1 & 0 & -N \\ a_{21} & 0 & 1 & -P_R \\ a_{31} & 0 & 1 & 0 \\ a_{41} & 1 & 0 & 0 \end{vmatrix} = (a_{11} - a_{41})P_R - (a_{21} - a_{31})N = 0, \quad (53)$$

which results in

$$(a_{11} - a_{41})P_R = (a_{21} - a_{31})N \quad (54)$$

By substituting values of a_{11} , a_{21} , a_{31} , and a_{41} in (54), the following equality is formed

$$\begin{aligned} \eta_0 N P_R^2 + (aM^2 + N^2 + 2aMN)P_R \\ - 2aMNP_T = 0. \end{aligned} \quad (55)$$

On the other hand, by substituting $P_S = P_T - P_R$ into C_1 in (46), obtained from C_2 , we have

$$\eta_0 N P_R^2 + (aM^2 + MN)P_R - aM^2 P_T = 0. \quad (56)$$

By setting

$$\begin{aligned} \alpha &= \eta_0 N, \\ b_1 &= aM^2 + N^2 + 2aMN, \\ c_1 &= 2aMNP_T, \\ b_2 &= aM^2 + MN, \\ c_2 &= aM^2 P_T, \end{aligned} \quad (57)$$

(55) and (56) can be written as

$$\alpha P_R^2 + b_1 P_R - c_1 = 0 \quad (58)$$

$$\alpha P_R^2 + b_2 P_R - c_2 = 0. \quad (59)$$

The roots of (58) and (59) are given as

$$P_{R,1} = \frac{-b_1 + \sqrt{4\alpha c_1}}{2\alpha} \quad (60)$$

$$P_{R,2} = \frac{-b_2 + \sqrt{4\alpha c_2}}{2\alpha}, \quad (61)$$

respectively. If we assume that $b_1 \ll 4\alpha c_1$ and $b_2 \ll 4\alpha c_2$ (due to the existence of η_0 in α), then (60) and (61) will be given as follows

$$P_{R,1} = \frac{\sqrt{4\alpha c_1}}{2\alpha} \quad (62)$$

$$P_{R,2} = \frac{\sqrt{4\alpha c_2}}{2\alpha}, \quad (63)$$

respectively. Since (62) and (63) need to be equal, we obtain

$$c_1 = c_2, \quad (64)$$

which results in

$$M = 2N. \quad (65)$$

Considering C_3 in (46), (65) gives us the optimal M , denoted by M^* , as

$$M^* = \frac{2K}{3}. \quad (66)$$

Substituting (66) in (62), we obtain the optimal P_R , denoted by P_R^* , as

$$P_R^* = \sqrt{\frac{4K\Omega_S N_0 P_T}{3\Omega_D \eta}}. \quad (67)$$

On the other hand, from C_2 and C_3 , we can obtain the optimal values of N and P_S , denoted by N^* and P_S^* , as

$$N^* = K - M^* = \frac{K}{3} \quad (68)$$

$$P_S^* = P_T - P_R^*. \quad (69)$$

This approximation is valid when

$$\begin{aligned} b_1^2 &\ll 4\alpha c_1, \\ b_2^2 &\ll 4\alpha c_2. \end{aligned} \quad (70)$$

One issue with the optimal result found for P_R , given by (67), is that when K grows to very large values, P_R^* becomes bigger than P_T which cannot happen. In order to solve this problem, we use $M^* = \frac{2K}{3}$ and $N^* = \frac{K}{3}$ as a starting point to maximize the rate. As a result, substituting $M^* = \frac{2K}{3}$ and $N^* = \frac{K}{3}$ in (43) leads to the following condition

$$\begin{aligned} &\frac{P_S \Omega_S \left(1 + \left(\frac{2K}{3} - 1\right)Q\right)}{N_0 + \frac{\eta}{M} P_R} \\ &= \frac{P_R \Omega_D \left(1 + \left(\frac{K}{3} - 1\right)Q\right)}{N_0}. \end{aligned} \quad (71)$$

In (71), we introduce the approximations, $1 + (2K/3 - 1)Q \approx 2KQ/3$ and $1 + (K/3 - 1)Q \approx KQ/3$, which become tight with increasing K and yields

$$\frac{P_S \Omega_S \left(\frac{2K}{3}Q\right)}{N_0 + \frac{\eta}{M} P_R} = \frac{P_R \Omega_D \left(\frac{K}{3}Q\right)}{N_0}. \quad (72)$$

Now, by substituting P_S with $P_T - P_R$, and solving the quadratic equation that results from the equality in (72) with respect to P_R , we obtain P_R^* and P_S^* given in (22) and (25), respectively.

APPENDIX C
PROOF OF COROLLARY 1

Let the fading channel between the source S and the m -th receive antenna of the relay be denoted by $h_{S,m}$, and is assumed to be a complex Gaussian random variable with zero mean and variance $\Omega_{S,m}$, i.e., $h_{S,m} \sim \mathcal{CN}(0, \Omega_{S,m})$. Let the fading channel between the n -th transmit antenna of the relay and the destination D be denoted by $h_{D,n}$, and is assumed to be a complex Gaussian random variable with zero mean and variance $\Omega_{D,n}$, i.e., $h_{D,n} \sim \mathcal{CN}(0, \Omega_{D,n})$. Therefore, the fading channels $h_{S,m}$ and $h_{D,n}$ can be expressed as

$$h_{S,m} = \alpha_m e^{j\phi_{S,m}}, \quad (73)$$

$$h_{D,n} = \beta_n e^{j\phi_{D,n}}, \quad (74)$$

where α_m and β_n are Rayleigh distributed channel gains between the source and the m -th receive antenna at the relay, and between and n -th transmit antenna at the relay and the destination, respectively. Hence, we have

$$f_{\alpha_m}(x) = \frac{2x}{\Omega_{S,m}} \exp\left(-\frac{x^2}{\Omega_{S,m}}\right), \quad x \geq 0 \quad (75)$$

$$f_{\beta_n}(x) = \frac{2x}{\Omega_{D,n}} \exp\left(-\frac{x^2}{\Omega_{D,n}}\right), \quad x \geq 0 \quad (76)$$

As a result of (75) and (76), $\mathbb{E}\{\alpha_m^2\} = \Omega_{S,m}, \forall m, \mathbb{E}\{\alpha_m\} = \sqrt{\Omega_{S,m}\pi/4}, \forall m$ and $\mathbb{E}\{\beta_n^2\} = \Omega_{D,n}, \forall n, \mathbb{E}\{\beta_n\} = \sqrt{\Omega_{D,n}\pi/4}, \forall n$. Due to the far field assumption, the average gain of the channel between the source and the m -th antenna element of the relay's receive array satisfies the following

$$\Omega_{S,m} = \Omega_S, \forall m. \quad (77)$$

Similarly, the average gain of the channel between the n -th antenna element of the relay's transmit array and the destination satisfies the following,

$$\Omega_{D,n} = \Omega_D, \forall n. \quad (78)$$

From (14), the SINR at the relay, denoted by γ_{SR}^{Ra} , can be obtained as

$$\gamma_{SR}^{Ra} \stackrel{(f)}{=} \frac{P_S \mathbb{E}_{\mathbf{h}_{SR}} \left\{ |\mathbf{u}^T \mathbf{h}_{SR}|^2 \right\}}{\mathbb{E}_{\mathbf{w}_R} \left\{ |\mathbf{u}^T \mathbf{w}_R|^2 \right\} + P_R \mathbb{E}_{\mathbf{G}} \left\{ \left| \sqrt{\frac{1}{N}} \mathbf{u}^T \mathbf{G} \mathbf{v} \right|^2 \right\}}, \quad (79)$$

where (f) results from $E_{x_S} \{|x_S|^2\} = P_S$ and $E_{x_R} \{|x_R|^2\} = P_R$. On the other hand, the only term in (79) different from (34) is $\mathbb{E}_{\mathbf{h}_{SR}} \left\{ |\mathbf{u}^T \mathbf{h}_{SR}|^2 \right\}$ which can be obtained as

$$\begin{aligned} & \mathbb{E} \left\{ |\mathbf{u}^T \mathbf{h}_S|^2 \right\} \\ &= \mathbb{E} \left\{ \left| \sum_{m=1}^M \alpha_m e^{j\hat{\phi}_{S,m}} e^{-j\hat{\phi}_{S,m}} \right|^2 \right\} \\ &= \mathbb{E} \left\{ \left| \sum_{m=1}^M \alpha_m e^{j\bar{\phi}_{S,m}} \right|^2 \right\} = \mathbb{E} \left\{ \sum_{m=1}^M \alpha_m^2 \right\} \\ &+ \mathbb{E} \left\{ \sum_{m=1}^M \sum_{j=1, j \neq m}^M \alpha_m \alpha_j e^{j\bar{\phi}_{S,m}} e^{-j\bar{\phi}_{S,j}} \right\}. \end{aligned} \quad (80)$$

(81) can be further simplified as

$$\begin{aligned}
& \mathbb{E} \left\{ \left| \mathbf{u}^T \mathbf{h}_S \right|^2 \right\} \\
&= \sum_{m=1}^M \mathbb{E} \left\{ \alpha_m^2 \right\} + \sum_{m=1}^M \sum_{j=1, j \neq m}^M \mathbb{E} \left\{ \alpha_m \right\} \\
&\quad \times \mathbb{E} \left\{ \alpha_j \right\} \mathbb{E} \left\{ e^{j\bar{\phi}_{S,m}} \right\} \mathbb{E} \left\{ e^{-j\bar{\phi}_{S,j}} \right\} \\
&= M\Omega_S \left(1 + (M-1) \frac{\pi}{4} Q \right), \tag{81}
\end{aligned}$$

where $\bar{\phi}_{S,m} = \phi_{S_m} - \hat{\phi}_{S_m}$ is the quantization noise (error) introduced by b -bit phase shifters at the relay's receiving antennas with $\mathbb{E} \left\{ e^{j\bar{\phi}_{S,m}} \right\} = \mathbb{E} \left\{ e^{-j\bar{\phi}_{S,m}} \right\} = \frac{2^b}{\pi} \sin \left(\frac{\pi}{2^b} \right) = \sqrt{Q}$. Hence, γ_{SR}^{Ra} is given by

$$\gamma_{SR}^{Ra} = \frac{P_S \Omega_S \left(1 + (M-1) \frac{\pi}{4} Q \right)}{N_0 + \frac{\eta}{N} P_R}. \tag{82}$$

On the other hand, the received SINR at the destination, denoted by γ_{RD}^{Ra} , is given by

$$\gamma_{RD}^{Ra} = \frac{P_R \left\{ |x_R|^2 \right\} \mathbb{E}_{\mathbf{h}_D} \left\{ \left| \frac{1}{\sqrt{N}} \mathbf{v}^T \mathbf{h}_D \right|^2 \right\}}{\mathbb{E}_{w_D} \left\{ w_D^2 \right\}}, \tag{83}$$

where the only term in (83) different from (40) is $\mathbb{E}_{\mathbf{h}_{RD}} \left\{ \left| \frac{1}{\sqrt{N}} \mathbf{v}^T \mathbf{h}_{RD} \right|^2 \right\}$. After similar derivations to (81), we obtain γ_{RD}^{Ra} as

$$\gamma_{RD}^{Ra} = \frac{P_R \Omega_D \left(1 + (N-1) \frac{\pi}{4} Q \right)}{N_0}. \tag{84}$$

As a result of (82) and (84), we can conclude that R_{Relay}^{Ra} is given by (27).

REFERENCES

- [1] C. Liaskos, S. Nie, A. Tsioliaridou, A. Pitsillides, S. Ioannidis, and I. Akyildiz, "A new wireless communication paradigm through software-controlled metasurfaces," *IEEE Communications Magazine*, vol. 56, no. 9, pp. 162–169, 2018.

- [2] Z. Hadzi-Velkov, S. Pejoski, N. Zlatanov, and H. Gačanin, "Designing wireless powered networks assisted by intelligent reflecting surfaces with mechanical tilt," *IEEE Communications Letters*, vol. 25, no. 10, pp. 3355–3359, 2021.
- [3] M. Di Renzo, K. Ntontin, J. Song, F. H. Danufane, X. Qian, F. Lazarakis, J. De Rosny, D. T. Phan-Huy, O. Simeone, R. Zhang, M. Debbah, G. Lerosey, M. Fink, S. Tretyakov, and S. Shamai, "Reconfigurable intelligent surfaces vs. relaying: Differences, similarities, and performance comparison," *IEEE Open Journal of the Communications Society*, vol. 1, pp. 798–807, 2020.
- [4] E. Björnson, Ö. Özdogan, and E. G. Larsson, "Intelligent reflecting surface versus decode-and-forward: How large surfaces are needed to beat relaying?" *IEEE Wireless Communications Letters*, vol. 9, no. 2, pp. 244–248, 2019.
- [5] L. Lu, G. Y. Li, A. L. Swindlehurst, A. Ashikhmin, and R. Zhang, "An overview of massive mimo: Benefits and challenges," *IEEE Journal of Selected Topics in Signal Processing*, vol. 8, no. 5, pp. 742–758, 2014.
- [6] E. G. Larsson, O. Edfors, F. Tufvesson, and T. L. Marzetta, "Massive mimo for next generation wireless systems," *IEEE Communications Magazine*, vol. 52, no. 2, pp. 186–195, 2014.
- [7] W. Roh, J.-Y. Seol, J. Park, B. Lee, J. Lee, Y. Kim, J. Cho, K. Cheun, and F. Aryanfar, "Millimeter-wave beamforming as an enabling technology for 5g cellular communications: theoretical feasibility and prototype results," *IEEE Communications Magazine*, vol. 52, no. 2, pp. 106–113, 2014.
- [8] A. F. Molisch, V. V. Ratnam, S. Han, Z. Li, S. L. H. Nguyen, L. Li, and K. Haneda, "Hybrid beamforming for massive mimo: A survey," *IEEE Communications Magazine*, vol. 55, no. 9, pp. 134–141, 2017.
- [9] F. Sohrabi and W. Yu, "Hybrid digital and analog beamforming design for large-scale antenna arrays," *IEEE Journal of Selected Topics in Signal Processing*, vol. 10, no. 3, pp. 501–513, 2016.
- [10] I. Ahmed, H. Khammari, A. Shahid, A. Musa, K. S. Kim, E. De Poorter, and I. Moerman, "A survey on hybrid beamforming techniques in 5g: Architecture and system model perspectives," *IEEE Communications Surveys Tutorials*, vol. 20, no. 4, pp. 3060–3097, 2018.
- [11] R. Méndez-Rial, C. Rusu, N. González-Prelcic, A. Alkhateeb, and R. W. Heath, "Hybrid mimo architectures for millimeter wave communications: Phase shifters or switches?" *IEEE Access*, vol. 4, pp. 247–267, 2016.
- [12] L. Yin, P. Yang, Y. Gan, F. Yang, S. Yang, and Z. Nie, "A low cost, low in-band rcs microstrip phased-array antenna with integrated 2-bit phase shifter," *IEEE Transactions on Antennas and Propagation*, vol. 69, no. 8, pp. 4517–4526, 2021.
- [13] Q. Wu and R. Zhang, "Towards smart and reconfigurable environment: Intelligent reflecting surface aided wireless network," *IEEE Communications Magazine*, vol. 58, no. 1, pp. 106–112, 2020.
- [14] J. Feng, S. Ma, G. Yang, and B. Xia, "Power scaling of full-duplex two-way massive mimo relay systems with correlated antennas and mrc/mrt processing," *IEEE Transactions on Wireless Communications*, vol. 16, no. 7, pp. 4738–4753, 2017.
- [15] H. Q. Ngo, H. A. Suraweera, M. Matthaiou, and E. G. Larsson, "Multipair full-duplex relaying with massive

- arrays and linear processing,” *IEEE Journal on Selected Areas in Communications*, vol. 32, no. 9, pp. 1721–1737, 2014.
- [16] A. Pizzo, T. L. Marzetta, and L. Sanguinetti, “Spatially-stationary model for holographic mimo small-scale fading,” *IEEE Journal on Selected Areas in Communications*, vol. 38, no. 9, pp. 1964–1979, 2020.
- [17] R. Deng, B. Di, H. Zhang, D. Niyato, Z. Han, H. V. Poor, and L. Song, “Reconfigurable holographic surfaces for future wireless communications,” *arXiv preprint arXiv:2112.06372*, 2021.
- [18] E. Björnson and L. Sanguinetti, “Power scaling laws and near-field behaviors of massive mimo and intelligent reflecting surfaces,” *IEEE Open Journal of the Communications Society*, vol. 1, pp. 1306–1324, 2020.
- [19] N. Zlatanov, E. Sippel, V. Jamali, and R. Schober, “Capacity of the gaussian two-hop full-duplex relay channel with residual self-interference,” *IEEE Transactions on Communications*, vol. 65, no. 3, pp. 1005–1021, 2017.
- [20] E. Everett, A. Sahai, and A. Sabharwal, “Passive self-interference suppression for full-duplex infrastructure nodes,” *IEEE Transactions on Wireless Communications*, vol. 13, no. 2, pp. 680–694, 2014.
- [21] O. Özdoğan, E. Björnson, and E. G. Larsson, “Intelligent reflecting surfaces: Physics, propagation, and pathloss modeling,” *IEEE Wireless Communications Letters*, vol. 9, no. 5, pp. 581–585, 2020.
- [22] S. W. Ellingson, “Path loss in reconfigurable intelligent surface-enabled channels,” in *2021 IEEE 32nd Annual International Symposium on Personal, Indoor and Mobile Radio Communications (PIMRC)*, 2021, pp. 829–835.
- [23] K. Ntontin, M. Di Renzo, and F. Lazarakis, “On the rate and energy efficiency comparison of reconfigurable intelligent surfaces with relays,” in *2020 IEEE 21st International Workshop on Signal Processing Advances in Wireless Communications (SPAWC)*, 2020, pp. 1–5.
- [24] V. V. Ratnam and A. F. Molisch, “Periodic analog channel estimation aided beamforming for massive mimo systems,” *IEEE Transactions on Wireless Communications*, vol. 18, no. 3, pp. 1581–1594, 2019.
- [25] V. V. Ratnam and A. F. Molisch, “Continuous analog channel estimation-aided beamforming for massive mimo systems,” *IEEE Transactions on Wireless Communications*, vol. 18, no. 12, pp. 5557–5570, 2019.
- [26] Q. Wu and R. Zhang, “Beamforming optimization for wireless network aided by intelligent reflecting surface with discrete phase shifts,” *IEEE Transactions on Communications*, vol. 68, no. 3, pp. 1838–1851, 2019.
- [27] N. Zlatanov, R. Schober, and P. Popovski, “Buffer-aided relaying with adaptive link selection,” *IEEE Journal on Selected Areas in Communications*, vol. 31, no. 8, pp. 1530–1542, 2012.